ADVANCED FUNCTIONAL MATERIALS

FULL PAPER

Tailored Macroporous SiCN and SiC Structures for High-Temperature Fuel Reforming**

By *In-Kyung Sung*, *Christian*, *Michael Mitchell*, *Dong-Pyo Kim*,* and *Paul J. A. Kenis**

The catalytic reforming of hydrocarbons in a microreformer is an attractive approach to supply hydrogen to fuel cells while avoiding storage and safety issues. High-surface-area catalyst supports must be stable above 800 °C to avoid catalyst coking; however, many porous materials lose their high surface areas below 800 °C. This paper describes an approach to fabricate macroporous silicon carbonitride (SiCN) and silicon carbide (SiC) monoliths with geometric surface areas of 10^5 to 10^8 m^2 per m^3 that are stable up to 1200 °C. These structures are fabricated by capillary filling of packed beds of polystyrene or silica spheres with low-viscosity preceramic polymers. Subsequent curing, pyrolysis, and removal of the spheres yielded SiCN and SiC inverted beaded monoliths with a chemical composition and pore morphology that are stable in air at 1200 °C. Thus, these structures are promising as catalyst supports for high-temperature fuel reforming.

1. Introduction

Porous solids with tailored pore characteristics have attracted considerable attention because of their many potential applications, including use as selective membranes,[1] photonic bandgap materials,[1] and waveguides.[2] In addition, high-surface-area porous solids are suitable as catalyst supports[3] for reactions such as the reforming of hydrocarbon fuels (e.g., diesel or JP-8) into hydrogen for use in portable power sources. Performing heterogeneous catalytic reactions in porous structures at the microscale has certain advantages. Heat and mass transfer fluxes are much larger at the microscale than those at the macroscale, as a result of the shorter distances and the larger surface-area-to-volume ratios.[4,5] Limitations in the heat transfer rate to the reactants that typically reduce the operating temperature, and therefore the reaction rate of endothermic reactions (such as the steam reforming of hydrocarbons), at the macroscale are avoided by operating at the microscale. In fact, microscale reactors with integrated heaters for steam reforming of methanol have already been reported.[6,7] Additionally, the use of monolithic porous structures within microchannels is preferred over the traditionally used packed particle beds. Packed particles settle as a result of vibrations and shock that are commonly encountered in portable devices. Flow of the reactants is diverted around the particles, called channeling, which reduces the conversion efficiency of the reaction.[8] This phenomenon is avoided when using a monolithic catalyst support.

The challenge in the fabrication of monolithic microscale catalyst support structures for high-temperature fuel reforming is to combine *within one structure* the following properties: i) a high surface area per unit volume to reduce the required reformer volume for a given conversion; ii) compatibility with high temperatures, ideally 800 °C or higher, to avoid coking[9,10] of the catalytic structure; and iii) an acceptable pressure drop. The requirement of a high surface area per unit volume can be met in a highly porous material with interconnected pores. Unfortunately, obtaining such porous structures that also fulfill the pressure-drop and thermal-compatibility requirements has proven to be difficult.

Many of the monolithic (i.e., non-particle-based) high-surface-area porous materials reported to date are oxides prepared by flame pyrolysis or sol–gel techniques,[11–15] or carbon molecular sieves with surface areas per unit volume of 10^9 m^2 per m^3 created from silica templates.[16,17] The poor stability of these materials, such as the hydrothermal instability of mesoporous zeolites at temperatures approaching 800 °C[12] and the complete combustion of carbon molecular sieves in air at 500 °C,[16] however, makes them inappropriate for the reforming of hydrocarbon fuels. Others have fabricated porous silica and titania structures with values of surface area per unit volume of between 10^5 and 10^8 m^2 per m^3 around a template, using either solid particles or supramolecular assemblies to form the template.[3,18,19] Unfortunately, all of these oxide materials lose their structural integrity below 800 °C, which limits

[*] Prof. D.-P. Kim, I.-K. Sung
Department of Fine Chemical Engineering and Chemistry
Chungnam National University
Daejeon, 305-764 (Korea)
E-mail: dpkim@cnu.ac.kr
Prof. P. J. A. Kenis, Christian, M. Mitchell
Department of Chemical and Biomolecular Engineering
University of Illinois at Urbana-Champaign
600 S. Mathews Ave., Urbana, IL 61801 (USA)
E-mail: kenis@uiuc.edu

[**] Financial support by the DoD Multidisciplinary University Research Initiative (MURI) administered by the Army Research Office under Grant DAAD19-01-1-0582, the campus research board of the University of Illinois, and the 2004 National Research Lab (NRL) project (project number M 10400000061-04J0000-06110) administered by the Korean Ministry of Science and Technology (MOST) is gratefully acknowledged. M. M. gratefully acknowledges the NSF for a graduate fellowship. SEM and XPS were carried out in the Center for Microanalysis of Materials, University of Illinois, which is partially supported by the U.S. Department of Energy under grant DEFG02-91-ER45439. The authors thank Q. D. Nghiem for his help with NMR and XRD analysis. Supporting Information is available online from Wiley InterScience or from the author.

  DOI: 10.1002/adfm.200500038

ADVANCED FUNCTIONAL MATERIALS

their applicability for fuel reforming of higher hydrocarbons, because higher temperatures are needed to eliminate coking.

In contrast, *non-oxide* materials, such as silicon nitride, are more promising owing to their chemical and thermal stability at higher temperatures (> 800 °C). For example, Huppertz and Schnick have synthesized nitridosilicates that have a zeolite-analogous silicon nitride structure with 1 nm pores, a thermal stability up to 1600 °C, and a surface area per unit volume value of the order of 10^9 m^2 per m^3.[20] This nanoporous structure, because of its small pores, would lead to large, unsustainable pressure drops within a reactor if used as a monolithic catalyst support. Moreover, methods to increase the pore size in these nitridosilicate structures,[20] and thereby decrease the pressure drop, are not (to the best of our knowledge) available.

Similarly, non-oxide materials such as silicon carbonitride (SiCN) and silicon carbide (SiC) exhibit high thermal and chemical stability, yet methods to obtain SiCN or SiC monoliths with tailored porous structures have not been reported to date. Recently, we reported the fabrication of macroporous SiCN and SiC as a powdery product using sacrificial templates.[21–23] Yang et al. have shown the fabrication of borosilicon carbonitride microscale structures via replica molding;[24] others have fabricated microscale structures that are stable over 1500 °C via photopolymerization of a liquid SiCN precursor.[25] Nanophase composites of SiC/Si_3N_4 have been synthesized by the carbothermal nitridation of silica, and the resulting composite powder has been used to make nonporous parts with excellent mechanical properties at temperatures as high as 1300 °C.[26]

Herein, we report the preparation of tailored, highly uniform SiCN and SiC porous structures, and validate their capability as catalyst support structures for high-temperature fuel reforming. We will show that these SiCN and SiC microstructured materials satisfy all three key requirements for the reforming of higher hydrocarbon fuels at the microscale: *geometric* surface areas per unit volume of the order of 10^5 to 10^8 m^2 per m^3 for pore diameters of 10 μm to 50 nm, porous features that are stable up to 1200 °C, and pressure drops that are realistic in magnitude for microscale systems.

2. Results and Discussion

Figure 1 shows the steps for fabricating the SiCN and SiC structures reported herein. For the synthesis of these tailored porous SiCN and SiC microchannel replicas, we adopted the MIMIC method used previously for the synthesis of porous oxide materials.[27] In short, a PDMS mold is placed onto a flat surface, here a chrome-coated silicon wafer, forming channels that are open at both ends. A solution containing either PS or silica (SiO_2) spheres is then allowed to flow slowly into the channels from one end by capillary action. Once the solution reaches the other end of the channel, the spheres begin to pack and the packing continues towards the inlet end. Growth of ordered domains of packed spheres occurs as the sphere solution flows toward the nucleation sites to replace the evaporated solvent at the outlet end.[27] After the packing process is completed, the solvent is removed completely, leaving behind a sacrificial template consisting of a close-packed bed of spheres.[27] Next, for the formation of the SiCN or SiC structures reported herein, we filled the void spaces between the spheres by capillary action with a preceramic polymer-based liquid: KiON Ceraset polyvinylsilazane (PVS) or allylhydridopolycarbosilane (AHPCS), respectively. Owing to the sensitivity of the preceramic polymers to moisture and O_2, the polymers were handled inside a glove box in a dry nitrogen atmosphere. The preceramic polymer, which also contained a small amount of thermal initiator, was then cured at 70 °C for 12 h under a nitrogen atmosphere. This low curing temperature enabled the use of a sacrificial template of packed PS spheres, which have a glass-transition temperature around 100 °C.[28] After removing the PDMS mold, the cured ceramic precursor was pyrolyzed at 1200 °C for two hours under an argon atmosphere. The PS spheres decomposed during the early stages of the pyrolysis process, whereas the SiO_2 spheres were etched away with a 10 vol.-% HF solution after pyrolysis. In both cases, depending on the preceramic polymer used, PVS or AHPCS, the result was a SiCN or SiC microchannel replica monolith, respectively, with a tailored, inverted beaded, porous structure. The higher void fraction ($\varepsilon = 0.74$) of an inverted beaded structure as opposed to a beaded structure ($\varepsilon = 0.26$) is a key advantage, as it results in a pressure drop per unit length about two orders of magnitude lower, as calculated using the Ergun equation.[8]

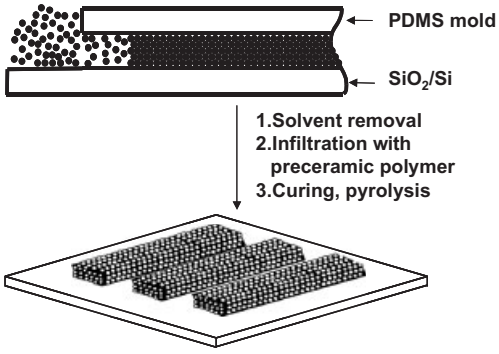

Figure 1. Schematic of the micromolding in capillaries (MIMIC)-based fabrication procedure as developed by Kim et al. [27] and applied here to the synthesis of SiCN and SiC macroporous structures. A packed bed of polystyrene (PS) spheres is formed inside a microfluidic channel (poly(dimethylsiloxane); PDMS) by evaporation-driven self-assembly [27]. An inverted beaded ceramic structure is obtained after infiltration of the beaded packed bed with a preceramic polymer, followed by curing and pyrolysis.

Figure 2 shows scanning electron microscopy (SEM) images taken at various fabrication stages of the inverted beaded SiCN and SiC porous monoliths using packed beds of PS or SiO_2 spheres as the sacrificial template. Highly ordered domains of packed spheres were formed (Fig. 2a), which are essential for obtaining the open, interconnected, porous structures required for the envisioned continuous-flow microreactor application. The quality of the resulting packed beds depends on the type of spheres used, their polydispersity, and the solvent used in the packing process. Packing of PS spheres from ethanol in-

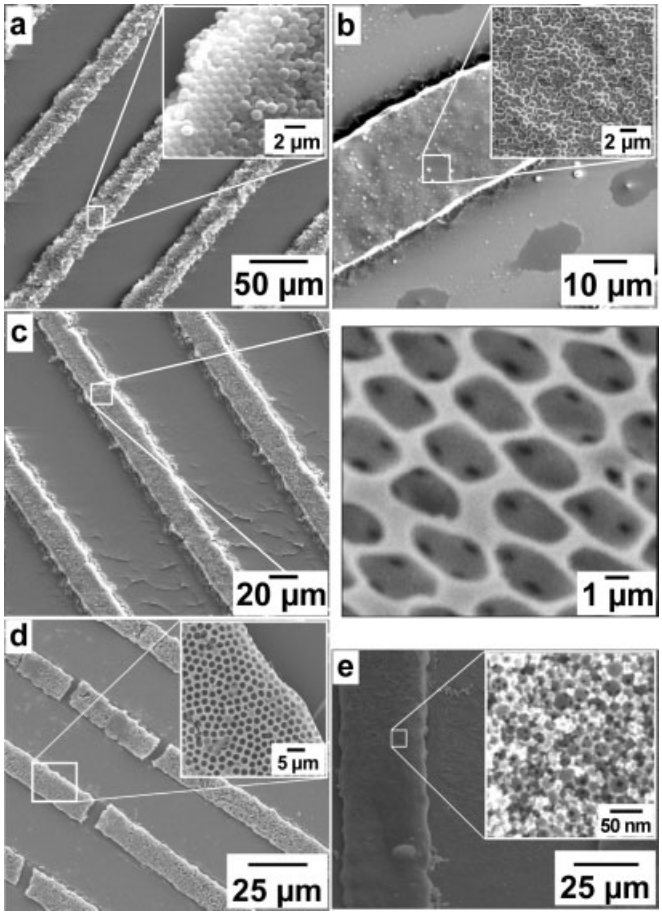

Figure 2. SEM micrographs showing the different stages of the fabrication process. a) Packed beds of 1 μm PS spheres in PDMS microchannels (20 μm × 8 μm). b) Packed beds of 1 μm PS spheres after infiltration with PVS and curing inside a 40 μm × 8 μm microchannel. c) SiCN microchannel replica and its three-dimensionally interconnected pore structure comprising 1 μm pores (magnified image on the right) formed by pyrolysis. d,e) Porous SiC monoliths with 1.5 μm and 40–50 nm pores, respectively, after pyrolysis and subsequent removal of the sacrificial SiO_2 spheres by etching with 10 % HF solution.

stead of water resulted in less-ordered structures, owing to the faster evaporation rate of ethanol. Additionally, quicker, pressure-assisted filling of the channel led to less-ordered packing, as expected. In general, the packing quality of SiO_2 spheres was lower than that of PS spheres because of the more rapid settling rates of the denser SiO_2 spheres.

Figure 2b shows a microchannel replica structure after infiltration of the void spaces between the PS spheres with the preceramic polymer PVS, followed by thermal curing. The void spaces within the sacrificial beaded template are essentially filled. When using packed beds of PS spheres as the sacrificial template, the spheres started to decompose at 300 °C during the pyrolysis step, leaving behind open, interconnected pores. After pyrolysis, a 1 mm long, crack-free SiCN microchannel replica with 1 μm uniform pores interconnected by 150–200 nm windows was obtained (Fig. 2c). Although the PS spheres are spherical, the resulting pores in the microstructure are elliptical and elongated in the channel flow direction. We attribute this distortion to higher stresses in the direction perpendicular to the channel walls. When we filled a channel with only preceramic polymer, a ceramic "rod" with many cracks was obtained after curing and pyrolysis, as a result of the expected 30 % shrinkage.[29] The spheres may, therefore, serve as a structural support during the early stages of pyrolysis by absorbing some of the shrinkage stresses. The lateral shrinkage observed within the porous structures further supports this explanation.

Figures 2d,e show SiC microchannel replicas with interconnected pores, as obtained using packed beds of 1.5 μm and 40–50 nm SiO_2 spheres, respectively, as the sacrificial template. The open, interconnected pores were obtained after etching in HF. Cracks are observed, however, in the microchannel replica structure due to excessive stresses between the harder, less compliant SiO_2 spheres and the ceramic precursor during the early stages of pyrolysis. The lower uniformity of the porous structure shown in Figure 2e can be explained by the larger dispersity (40–50 nm) of the SiO_2 spheres used, leading to packed beds with less-perfect packing.

Forming packed beds of PS or SiO_2 spheres by sedimentation of spheres from a solution in a PDMS tube, here ≈ 7 mm in diameter and ≈ 35 mm in height, provides a route to larger macroporous SiCN and SiC structures. After settling of the spheres, the top layer of water was removed and more sphere solution was added and allowed to settle. After packing of the spheres was completed, the same procedure as described above was followed for drying, infiltration, curing, and pyrolysis, to obtain cylindrical-shaped SiCN and SiC porous structures. This sedimentation approach, however, can lead to poorly packed beds compared to those obtained by the MIMIC-based packing procedure.

NMR spectroscopy and X-ray diffraction (XRD) were used to study the chemical and structural changes occurring during the conversion of the preceramic polymers to the ceramic products. Figures 3a,b show the ^{13}C NMR and ^{29}Si NMR spectra, respectively, for the PVS-derived ceramic as a function of pyrolysis temperature under a nitrogen atmosphere. When the samples were pyrolyzed at 950 °C or higher, the peaks in the ^{13}C NMR spectrum between –1 and 5 ppm (corresponding to the aliphatic carbons in the precursor), as well as the peaks between 132 and 142 ppm (corresponding to the vinyl carbons in the precursor) disappeared. A new, broad peak at ≈ 112 ppm represents an amorphous, graphite-like carbon phase in the amorphous ceramic. The ^{29}Si NMR spectrum shows shifting and broadening of the peak in the sample after pyrolysis at 950 °C, indicating that amorphous SiCN is being formed. The broad peak is due to the range of environments that the silicon atoms are in, depending on the number of bonds they have to carbon and nitrogen atoms. A lack of peaks in the XRD pattern for the pyrolyzed PVS (Fig. 4a) indicates the formation of an amorphous product after pyrolysis above 950 °C.

Figures 3c,d show the ^{13}C and ^{29}Si MAS NMR spectra, respectively, for the AHPCS-derived ceramic as a function of pyrolysis temperature under a nitrogen atmosphere. As the pyrolysis temperature was increased, the two peaks in both spectra of the precursor became one broad peak, indicating the

ADVANCED FUNCTIONAL MATERIALS

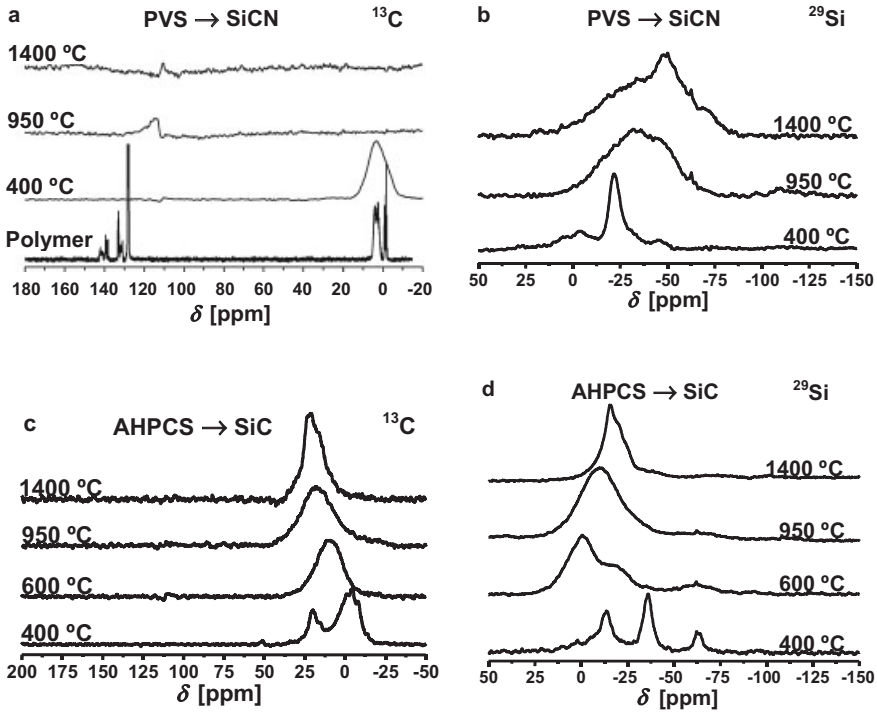

Figure 3. NMR spectra of the polymeric precursors pyrolyzed at different temperatures under a nitrogen atmosphere: a) ^{13}C NMR spectra; b) ^{29}Si NMR spectra for PVS-derived samples. c) ^{13}C magic angle spinning (MAS) NMR spectra; d) ^{29}Si MAS NMR spectra for AHPCS-derived samples.

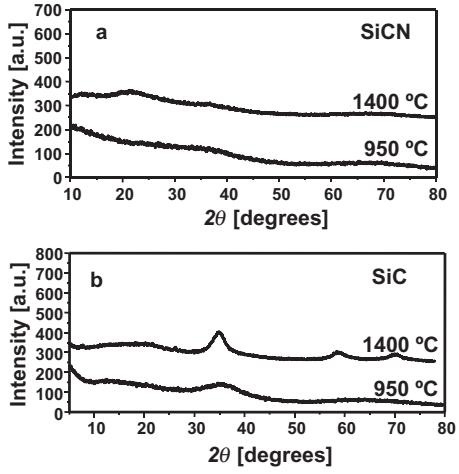

Figure 4. XRD patterns of a) SiCN and b) SiC bulk samples pyrolyzed at different temperatures under a nitrogen atmosphere.

formation of amorphous SiC from the AHPCS precursor. When the material was heated to 1400 °C, the single peak became narrower, owing to the formation of β-SiC crystallites. XRD of the AHPCS-derived ceramics supports this (Fig. 4b). Pyrolysis at 950 °C resulted in an amorphous material, while the narrowing of a peak at $2\theta = 35.6°$ for pyrolysis at 1400 °C indicates the existence of crystalline phases suspended in an amorphous matrix. The results are consistent with reports that pyrolysis of AHPCS and PVS in an inert atmosphere forms amorphous SiC and SiCN, respectively.[30] At 1250 °C, amorphous SiC forms β-SiC crystallites, and at 1450 °C, amorphous SiCN forms either β-SiC crystallites (in argon) or a mixed crystalline phase with β-SiC, α-Si_3N_4, and β-Si_3N_4 in a nitrogen atmosphere.[29,30] These crystalline materials are all stable up to 1800 °C in air and up to 2000 °C in inert atmospheres, making them ideal for high-temperature applications.[31] In summary, the XRD and NMR data show that the macroporous structures are composed of amorphous SiCN and SiC, unless heated to 1400 °C or above.

Next, we studied the chemical and physical stability of the SiCN and SiC porous structures at high temperatures in an oxidative, rather than an inert, environment. From thermogravimetric analysis (TGA; see Supporting Information) up to 950 °C (the limit of TGA apparatus) in air, we determined that the pyrolyzed SiCN and SiC structures did not experience any significant weight change: ≈0.09 wt.-% gain and ≈0.07 wt.-% loss, respectively. In addition, we compared the composition and morphology of both SiCN and SiC samples that were just prepared by pyrolysis under an argon atmosphere, and after subsequent exposure to air at 1200 °C for 6 h. X-ray photoelectron spectroscopy (XPS) was used to determine the chemical composition, that is, the fraction of silicon present as carbide, nitride, oxide, and oxycarbide, of the SiCN and SiC porous structures. Comparison of the XPS analyses of structures "before" and "after" thermal treatment in air showed that the oxide content did not increase (Table 1), which indicates that the chemical composition of these structures is thermally stable up to at least 1200 °C in an oxidative environment. In addition, the morphology of the pores in the macroporous SiCN and SiC structures was studied by SEM. SEM micrographs showed that the morphology of both SiCN and SiC structures did not change upon heating at 1200 °C for 6 h in air (Fig. 5). In both samples, ordered pores interconnected with their neighbors via ≈200 nm windows can be ob-

Table 1. Chemical composition of SiCN and SiC porous structures before and after heat treatment at 1200 °C for 6 h under an air atmosphere, as obtained from the XPS spectra.

Chemical species	SiCN		SiC	
	Before heat treatment [%]	After heat treatment [%]	Before heat treatment [%]	After heat treatment [%]
SiC	19.0 ± 7.1	16.2 ± 2.5	88.1 ± 2.6	87.2 ± 1.3
Si_3N_4	60.5 ± 10.4	65.6 ± 2.1	–	–
SiOC	15.1 ± 3.7	12.7 ± 3.3	10.6 ± 2.3	11.9 ± 1.5
SiO_2	5.4 ± 1.8	5.5 ± 1.4	1.3 ± 0.4	0.9 ± 0.2

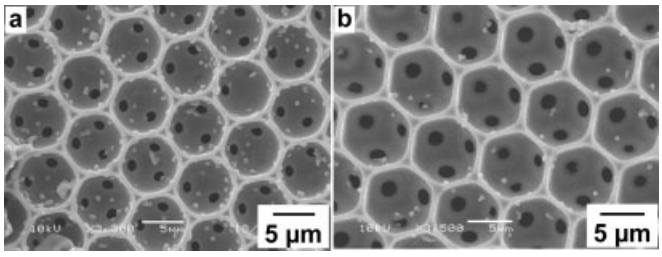

Figure 5. SEM micrographs of a) SiCN and b) SiC porous structures after heating at 1200 °C for 6 h in air. The little bits of debris on the surface of the porous structures are due to the cutting of the samples before SEM analysis.

served. TGA, XPS, and SEM data thus confirm that the macroporous SiCN and SiC structures reported herein are physically and chemically stable in air, at temperatures as high as 1200 °C.

The difference in packing quality between the structures shown in Figure 5 is a result of the poor control over packing quality when using the hard-to-control sedimentation method. In other experiments (Fig. 2c), highly ordered SiCN structures were obtained from beds of PS spheres with a much higher packing quality when prepared by the MIMIC-based packing procedure. At this point, it is also important to note that the morphological stability of these structures at high temperatures depends highly on their chemical composition. The pore morphology of samples that were not carefully kept in an inert and dry atmosphere during processing did undergo morphological changes upon heating: the inverted beaded structures started to collapse, interconnecting windows closed up, walls thickened, and amorphous regions appeared. XPS analysis confirmed that these structures contained large amounts of oxides, which led to sintering of the porous features. Maintaining dry and oxygen-free conditions during processing is thus key in obtaining morphologically stable macroporous SiCN and SiC structures, such as those shown in Figure 5.

The previous discussion shows that the macroporous SiCN and SiC structures fulfill the high-thermal-stability requirements for application as a catalyst support in fuel reforming. The second requirement of high surface area is also fulfilled: the geometric surface areas per unit volume are of the order of 10^5 to 10^8 m^2 per m^3 for pore diameters of 10 μm to 50 nm. Owing to nanoscale surface roughness, the actual surface areas of porous structures are expected to be higher, as we have previously shown experimentally.[22,23] The porous structures reported herein are presently too small to obtain a reliable value for the surface area using the Brunauer–Emmett–Teller (BET) method.

The last requirement—having a reasonable pressure drop, i.e., one that does not lead to material failure—can also be met: a pressure drop of only 0.008 atm (1 atm ≈ 10^5 Pa) was calculated for a 2 mm tall cylindrical SiCN or SiC monolith with a diameter of 7 mm and 10 μm pores using the Ergun equation,[8] while assuming temperature, $T = 500$ °C, and a flow rate of 40 sccm NH_3 at 1 atm, the conditions of our ammonia decomposition experiments described below. Reducing the pore size to 1 μm would lead to a pressure drop of only 0.5 atm. The pressure drop for these highly porous, inverted beaded SiCN and SiC structures is thus easily within limits that can be sustained within ceramic microstructures. Moreover, inverted beaded macroporous SiCN and SiC monoliths with pore diameters between 10 μm and 50 nm have pressure drops that are 10^8 to 10^3 times less than those for the zeolite-analogous nitridosilicate structure described earlier.[20]

After establishing that the SiCN and SiC porous structures fulfill all three key requirements for use as a catalyst support for fuel reforming, we tested them. Ruthenium was deposited on 7 mm cylindrical monoliths of porous SiCN and SiC via wet impregnation using a ruthenium(III) acetylacetonate solution,[32] followed by calcination and reduction in hydrogen to convert the ruthenium to the metallic form. We confirmed the presence of ruthenium on the macroporous structures both on the outer surface as well as in their interior (fracture profile) by XPS analysis. As the catalyst-loading procedure was not optimized, the atomic concentration of ruthenium on the outer surface of the cylindrical monoliths was about 40 times higher than that on the interior surface of the monoliths. To demonstrate the use of these monoliths as catalyst supports, the cylindrical SiCN and SiC porous structures were incorporated within a stainless steel housing and the decomposition of NH_3 was carried out at temperatures up to 500 °C. Figure 6 shows the conversion of NH_3 as a function of flow rate for temperatures between 350 and 500 °C. The solid lines in the graph fit the

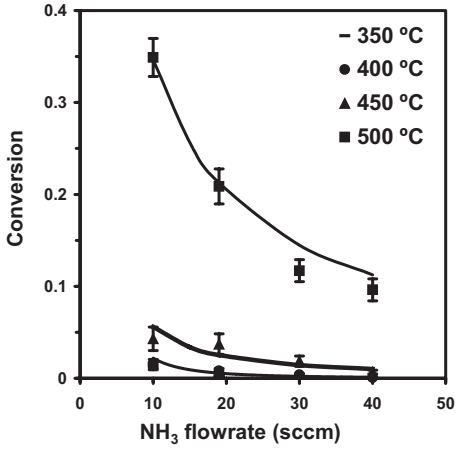

Figure 6. Graph showing the conversion of NH_3 as a function of NH_3 flow rate for different temperatures using a SiC porous structure as a catalyst support. The conversion of NH_3 was measured in 50 °C increments, from 350 to 500 °C (the temperature limit of the present testing setup). The NH_3 flow rates of 10 to 40 sccm correspond to residence times of 120 to 30 ms. The data obtained at 350 and 400 °C overlap.

conversion data assuming plug flow, constant temperature, no pressure drop, and first-order kinetics with respect to NH_3. As expected, conversion increases with longer residence times (lower flow rates) and with increasing temperature. These experiments were limited to 500 °C because stainless steel is known to catalyze NH_3 decomposition at higher temperatures,[33] making it difficult to separate the conversion due to

ADVANCED FUNCTIONAL MATERIALS

steel catalysis from the overall conversion. Once these porous SiCN and SiC catalyst support structures are integrated within high-temperature-stable housings, conversion data for fuel reforming at temperatures as high as 1200 °C can be obtained. The generation of hydrogen is expected to be much higher at higher temperatures, owing to faster reaction kinetics and higher equilibrium conversion, and lower residence times will be needed to attain complete conversion using SiCN or SiC porous structures. This work is ongoing.

3. Conclusion

For the first time, ceramic monoliths consisting of highly interconnected inverted beaded networks of uniform pores with diameters of 50 nm to 10 μm were obtained in the non-oxide materials of SiCN and SiC. The overall dimensions of these monoliths can be precisely tailored by the dimensions of the PDMS mold used; the pore size can be tailored *independently* by the bead size used within the packed beds that serve as the sacrificial template. The resulting macroporous SiCN and SiC structures retain both their chemical compositions and pore morphologies, even after exposure to an oxidative environment at 1200 °C for 6 h, as shown by XPS (Table 1) and SEM (Fig. 5) data. The structures are thus compatible with operation at temperatures above 800 °C, the temperature above which coking does not occur during the reforming of hydrocarbon fuels.

The crack-free, porous monoliths made of SiCN or SiC fulfill all three key requirements of catalyst supports for hydrocarbon reforming: a high surface area per unit volume is obtained through an interconnected network of uniform pores of nanometer to micrometer dimensions; compatibility with temperatures above 800 °C is achieved by using the thermally stable non-oxide materials of SiCN and SiC; and a low pressure drop while maintaining a high surface area is obtained by having an inverted beaded bed structure to form the network of interconnected pores with a porosity exceeding 0.7. Using the inverted beaded bed structure also eliminates channeling problems that occur with packed particle beds. The problem of coking of the catalyst while reforming higher hydrocarbons below 800 °C,[10] which to date has held back the development of microscale devices for the reforming of higher hydrocarbons, is expected to be eliminated by the use of these SiCN and SiC porous catalyst support structures, which are compatible with temperatures above 800 °C. These novel porous materials thus show great promise for microreactors for the on-demand reforming of higher hydrocarbons such as diesel and JP-8 into hydrogen for portable power sources. Currently, we are working to integrate these structures within a non-porous ceramic housing, enabling us to reform fuels at high temperatures.

4. Experimental

Microchannel Structures: PDMS molds with microchannel structures were produced by replica molding of a master obtained through photolithography, as described previously [34].

Creating Packed Beds of Beads: Solutions of PS spheres (0.06 to 10 μm in diameter; Polysciences) were obtained by mixing the PS bead solution (1 mL) with surfactant (0.1 mL, 5 wt.-%; Pluronic P123, BASF) in deionized water. Solutions of SiO_2 spheres (1.5 and 0.5 μm in diameter) were prepared by adding of spheres (3 g; Lancaster) to ethanol (10 mL), followed by sonication for 40 min (Branson 3510). Solutions of nanometer-sized spheres (Snowtex 50L, 20L, and ZL, with diameters of 20–30 nm, 40–50 nm, and 70–100 nm, respectively) were used as received. A drop of a PS- or silica-sphere solution (5–10 μL) was placed at one end of the channels of different dimensions (20–80 μm wide, 2–8 μm high, and 5–7 mm long), and left for 12 h to complete the packing process [27].

Creating Inverted Beaded Structures of SiCN and SiC: The SiCN and SiC precursor solutions consisted of 3–5 wt.-% of the thermal initiator 1,1-bis(tert-butylperoxy)-3,3,5-trimethylcyclohexane (92 %, Aldrich) in polyvinylsilazane (KiON Ceraset VL20, KiON Corporation), or in allylhydridopolycarbosilane (SP matrix, Starfire Systems), respectively. In some cases, the viscosity of the SP matrix mixture was lowered by dilution with tetrahydrofuran (THF) to facilitate infiltration. Infiltration of the packed beds of spheres with the precursor mixtures and curing of the mixtures was carried out in a glove box under a nitrogen atmosphere. After curing at 70 °C for 12 h, the PDMS mold was peeled away or removed by dissolution in tetrabutylammonium fluoride (1.0 M; TBAF) in THF for 20 min. Pyrolysis was carried out in a tube furnace (HTF5500 Series, Lindberg/Blue M) under an argon atmosphere by heating at 2 °C min^{-1} to 1200 °C and holding at 1200 °C for 2 h. Alternatively, packed beds were created by sedimentation of spheres within a PDMS tube (inner diameter 7 mm), followed by the same infiltration, curing, and pyrolysis steps as discussed above.

Structure Characterization: ^{13}C and ^{29}Si NMR measurements were carried out using a Bruker DMX600; ^{13}C and ^{29}Si MAS NMR experiments were performed on an FT Wide Bore (600 MHz) Unityl NOVA600 instrument. The pyrolyzed specimens were characterized by powder X-ray diffraction (Rigaku Miniflex) using Cu Kα radiation. TGA (TGA7, Perkin-Elmer) was performed by heating at 5 °C min^{-1} to 950 °C and holding at 950 °C for 30 min in air. The thermal stability of the porous structures was determined by heating the samples in a tube furnace (HTF5500 Series, Lindberg/Blue M) at 1200 °C for 6 h in air. XPS analysis was carried out using a PHI 5400 XPS (Physical Electronics) with an Mg Kα X-ray source. SEM micrographs were taken using either a Hitachi S-4700 or a JEOL 6060-LV scanning electron microscope.

Catalyst Deposition: The ruthenium catalyst was deposited on the SiC porous structure by impregnation with 0.96 wt.-% ruthenium(III) acetylacetonate (97 %, Aldrich) in 2,4-pentanedione (99+%, Aldrich) [32]. After drying, the structure was calcined in air at 580 °C in the tube furnace for 3 h. The structure was then mounted inside a stainless-steel holder using ceramic binder (Ceramabond 569, Aremco) and placed within a stainless-steel test fixture in the tube furnace. The catalyst was then reduced using 10 % H_2 in argon at 500 °C for 5 h. Reactants and products were led into and out of the test fixture through stainless steel tubing attached with Swagelok connections.

Fuel Reforming Tests: The flow of NH_3 (anhydrous, Matheson Gas Products) through the porous structure inside the test fixture was controlled using a mass flow controller (1479A MassFlo Controller, MKS Instruments), while the temperature of the test fixture with mounted porous structure was controlled inside the tube furnace. Gas chromatography/mass spectrometry (TRACE DSQ Single Quadrupole GC/MS, Thermo Finnigan) was used to measure the conversion of NH_3 into N_2 and H_2. For each flow rate of NH_3, the conversion data was taken after increasing the temperature of the furnace from 350 to 500 °C in 50 °C increments. The average conversion and its standard deviation were obtained from at least three measurements after steady-state operation was reached.

Received: December 23, 2004
Final version: March 20, 2005
Published online: July 1, 2005

[1] B. Gates, Y. Xia, *Adv. Mater.* **2000**, *12*, 1329.
[2] S. H. Park, Y. Xia, *Chem. Mater.* **1998**, *10*, 1745.

[3] B. Gates, Y. Yin, Y. Xia, *Chem. Mater.* **1999**, *11*, 2827.
[4] T. A. Ameel, R. O. Warrington, R. S. Wegeng, M. K. Drost, *Energy Convers. Manage.* **1997**, *38*, 969.
[5] K. F. Jensen, *AIChE J.* **1999**, *45*, 2051.
[6] A. V. Pattekar, M. V. Kothare, *J. Microelectromech. Syst.* **2004**, *13*, 7.
[7] J. D. Holladay, E. O. Jones, M. Phelps, J. Hu, *J. Power Sources* **2002**, *108*, 21.
[8] H. S. Fogler, *Elements of Chemical Reaction Engineering*, Prentice Hall, Englewood Cliffs, NJ **1999**.
[9] L. R. Arana, S. B. Schaevitz, A. J. Franz, K. F. Jensen, M. A. Schmidt, *Proc. Annu. Int. Conf. Micro Electro Mech. Syst., 15th* **2002**, 232.
[10] J. N. Armor, D. J. Martenak, *Appl. Catal., A* **2001**, *206*, 231.
[11] J. Weitkamp, *Solid State Ionics* **2000**, *131*, 175.
[12] A. Corma, *Chem. Rev.* **1997**, *97*, 2373.
[13] O. D. Velev, T. A. Jede, R. F. Lobo, A. M. Lenhoff, *Nature* **1997**, *389*, 447.
[14] J. E. G. J. Wijnhoven, W. L. Vos, *Science* **1998**, *281*, 802.
[15] G. Subramania, K. Constant, R. Biswas, M. M. Sigalas, K.-M. Ho, *Appl. Phys. Lett.* **1999**, *74*, 3933.
[16] R. Ryoo, S. H. Joo, S. Jun, *J. Phys. Chem. B* **1999**, *103*, 7743.
[17] S. B. Yoon, H. Y. Kim, J.-S. Yu, *Chem. Commun.* **2001**, 559.
[18] P. Yang, A. H. Rizvi, B. Messer, B. F. Chmelka, G. M. Whitesides, G. D. Stucky, *Adv. Mater.* **2001**, *13*, 427.
[19] M. Trau, N. Yao, E. Kim, Y. Xia, G. M. Whitesides, I. A. Aksay, *Nature* **1997**, *390*, 674.
[20] H. Huppertz, W. Schnick, *Angew. Chem., Int. Ed.* **1997**, *36*, 2651.
[21] I.-K. Sung, S.-B. Yoon, J.-S. Yu, D.-P. Kim, *Chem. Commun.* **2002**, 1480.
[22] H. Wang, S.-Y. Zheng, X.-D. Li, D.-P. Kim, *Microporous Mesoporous Mater.* **2005**, *80*, 357.
[23] H. Wang, X.-D. Li, J.-S. Yu, D.-P. Kim, *J. Mater. Chem.* **2004**, *14*, 1383.
[24] H. Yang, P. Deschatelets, S. T. Brittain, G. M. Whitesides, *Adv. Mater.* **2001**, *13*, 54.
[25] L.-A. Liew, Y. Liu, R. Luo, T. Cross, L. An, V. M. Bright, M. L. Dunn, J. W. Daily, R. Raj, *Sens. Actuators, A* **2002**, *95*, 120.
[26] A. W. Weimer, R. K. Bordia, *Composites, Part B* **1999**, *30*, 647.
[27] E. Kim, Y. Xia, G. M. Whitesides, *J. Am. Chem. Soc.* **1996**, *118*, 5722.
[28] www.polysciences.com/shop/assets/datasheets/238.pdf
[29] www.ceraset.com
[30] E. Kroke, Y.-L. Li, C. Konetschny, E. Lecomte, C. Fasel, R. Riedel, *Mater. Sci. Eng., R* **2000**, *26*, 97.
[31] www.starfiresystems.com
[32] J. C. Ganley, E. G. Seebauer, R. I. Masel, *J. Power Sources* **2004**, *137*, 53.
[33] W. Arabczyk, J. Zamlynny, *Catal. Lett.* **1999**, *60*, 167.
[34] D. C. Duffy, J. C. McDonald, O. J. A. Schueller, G. M. Whitesides, *Anal. Chem.* **1998**, *70*, 4974.

